CARTILAGE
2021, Vol. 13(Suppl 2) 419S–426S

DOI: 10.1177/1947603520968875
journals.sagepub.com/home/CAR
SAGE

The Effect of Overexpression of Lrp5 on the Temporomandibular Joint

Achint Utreja[1,2], Hengameh Motevasel[2], Carol Bain[3], Robert Holland[2], and Alexander Robling[4]

Abstract

Objective. The temporomandibular joint (TMJ) is a unique fibrocartilaginous joint that adapts to mechanical loading through cell signaling pathways such as the Wnt pathway. Increased expression of low-density lipoprotein receptor-related protein 5 (Lrp5), a co-receptor of the Wnt pathway, is associated with a high bone mass (HBM) phenotype. The objective of this study was to analyze the effect of overexpression of Lrp5 on the subchondral bone and cartilage of the TMJ in mice exhibiting the HBM phenotype. *Design*. Sixteen-week-old Lrp5 knock-in transgenic mice carrying either the A214V (EXP-A) or G171V (EXP-G) missense mutations, and wildtype controls (CTRL) were included in this study. Fluorescent bone labels, calcein, alizarin complexone, and demeclocycline were injected at 3.5, 7.5, and 11.5 weeks of age, respectively. The left mandibular condyle was used to compare the subchondral bone micro-computed tomography parameters and the right TMJ was used for histological analyses. Cartilage thickness, matrix proteoglycan accumulation, and immunohistochemical localization of Lrp5 and sclerostin were compared between the groups. *Results*. Subchondral bone volume (BV) and percent bone volume (BV/TV) were significantly increased in both EXP-A and EXP-G compared with CTRL ($P < 0.05$) whereas trabecular spacing (Tb.Sp) was decreased. Cartilage thickness, extracellular matrix production, and expression of Lrp5 and Sost were all increased in the experimental groups. The separation between the fluorescent bone labels indicated increased endochondral maturation between 3.5 and 7.5 weeks. *Conclusions*. These data demonstrate that Lrp5 overexpression leads to adaptation changes in the mandibular condylar cartilage of the TMJ to prevent cartilage degradation.

Keywords

temporomandibular joint, Wnt, Lrp5, chondrocytes

Introduction

The temporomandibular joint (TMJ) is an integral component of the masticatory system in mammals as it provides bilateral articulation between the temporal bone in the skull and the mandible. Development and function of the joint are regulated by interactions between various signal transduction pathways, including bone morphogenetic protein (BMP),[1] fibroblast growth factor (FGF),[2] Hedgehog,[3] Notch,[4] and Wnt/β-catenin.[5] Among these, the Wnt/β-catenin signaling pathway is composed of secreted glycoprotein molecules that play important roles during development and function.[6] At the cellular level, Wnt proteins play a role in cell fate determination. When the pathway is suppressed, osteoblast precursor cells have been shown to differentiate into chondrocytes.[7] The Wnt pathway is also an important mediator of mechanical loading-induced cellular and molecular responses in components of the musculoskeletal system such as bone and cartilage.[8] The activated pathway orchestrates an anabolic remodeling response in mechanically stimulated skeletal tissues.[9] Changes in the expression of Wnt-related genes in cultured mesenchymal stem cells subjected to dynamic loading, have been observed.[10] During the formation of cartilaginous joints, the Wnt pathway regulates joint patterning and chondrocyte maturation by responding to mechanical stimuli.[5]

The low-density lipoprotein-related receptor-5 (Lrp5) is a prominent member of the family of receptor complexes that bind to Wnt proteins.[6] Alterations in the activity and expression of Lrp5 affect Wnt-regulated bone remodeling.

[1]Section of Orthodontics, Department of Growth, Development and Structure, Southern Illinois University School of Dental Medicine, Alton, IL, USA
[2]Department of Orthodontics and Oral Facial Genetics, Indiana University School of Dentistry, Indianapolis, IN, USA
[3]Histotechnology Program, Indiana University School of Medicine, Indianapolis, IN, USA
[4]Department of Anatomy and Cell Biology, Indiana University School of Medicine, Indianapolis, IN, USA

Corresponding Author:
Achint Utreja, Section of Orthodontics, Department of Growth, Development and Structure, Southern Illinois University School of Dental Medicine, 2800 College Avenue, Alton, IL 62002, USA.
Email: autreja@siue.edu

Both loss- and gain-of-function mutations of Lrp5 have been utilized to study this protein in detail. In transgenic mice engineered with a loss-of-function mutation in Lrp5 ($Lrp5^{-/-}$), bone mineral density (BMD) and bone strength were reduced, leading to a decreased osteogenic response to mechanical loading in these animals.[11] On the other hand, a gain-of-function mutation in the LRP5 gene in humans led to a high bone mass (HBM) condition that is characterized by a significant increase in BMD.[12] To better understand the HBM phenotype, 2 knock-in mouse lines with separate gain-of-function missense mutations in Lrp5, have been generated. Phenotypically, both the A214V and the G171V lines of mutant mice were shown to have high bone mass, increased BMD and improved biomechanical properties.[13]

Although the role of Lrp5 in mediating an anabolic bone remodeling response in the appendicular skeleton has been elucidated, there is little information about its effect on the craniofacial skeleton. The periosteum-derived mandibular condylar cartilage (MCC) of the TMJ[14] is the ideal model to analyze this as it relies on mechanical stimulation for development and function and has an interface of fibrocartilage and bone. Thus, the *objective* of this study was to compare the effect of two distinct Lrp5-HBM mutations on the mandibular condylar cartilage and underlying subchondral bone of the TMJ. The *hypothesis* was that a gain-of-function mutation of Lrp5 decreases condylar cartilage thickens and increases subchondral bone mass in the mandibular condyle.

Materials and Methods

Study Design

A total of thirty 16-week-old male mice were used for this study. Of these, 20 transgenic mice were equally divided into 2 experimental groups (EXP-A, EXP-G; $n = 10$/group) and 10 wildtype mice were included in the control group (CTRL). The experimental animals carried gain-of-function HBM Wnt signaling pathway mutations: $Lrp5^{G171V/G171V}$ and $Lrp5^{A214V/A214V}$. The generation of these knock-in mutant lines has been described previously.[15] All mice, including the widltype controls were on a mixed genetic background of 129S1/SvIMJ and C57Bl/6J.

All experimental procedures were performed according to a protocol approved by the Institutional Animal Care and Use Committee (IACUC). The animals were housed in standard light and dark conditions and were fed pellet diet and water *ad libitum*. Fluorescent bone labels, calcein, alizarin complexone, and demeclocycline (Sigma-Aldrich, St. Louis, MO) were injected intraperitoneally at 3.5, 7.5, and 11.5 weeks of age, respectively. At 16 weeks of age, mice in all 3 groups were euthanized by CO_2 inhalation.

Tissue Collection

On the right side of the skull, the TMJ was dissected *en masse* (mandibular condyle, articular disc, and temporal bone) after removing the skin and superficial muscles. On the left side, the mandibular condyle was isolated and dissected by removing all the surrounding soft tissues. Both the TMJ and the mandibular condyle were fixed in 10% neutral buffered formalin for 3 days and then stored in 70% ethanol.

Micro-Computed Tomography

The mandibular condyles were scanned with a Skyscan 1172 (Bruker microCT, Kontich, Belgium) micro-computed tomography (micro-CT) scanner to analyze the subchondral bone and calcified cartilage. Serial tomographic slices were acquired at a resolution of 6 μm/pixel followed by reconstruction of 3-dimensional images using the NRecon software (v1.6.9.1). Volumetric analyses were then carried out with the CT-Analyser (CTAn version 1.13) software by selecting a region of interest (ROI) in the subchondral bone underlying the MCC (**Fig. 1A** and **B**). Micro-CT parameters, including bone volume (BV), total volume (TV), percent bone volume (BV/TV), trabecular number (Tb.N), trabecular separation (Tb.Sp), and trabecular thickness (Tb.Th) were compared between the groups.

Histology

For histological staining and imaging, the dissected and fixed TMJs were decalcified in a 10% EDTA (ethylenediaminetetraacetic acid) solution. The tissues were then processed in increasing concentrations of ethanol and xylene and embedded in paraffin. Serial sagittal sections of the joint were obtained with a rotary microtome (Leica Biosystems, Buffalo Grove, IL) and placed on positively charged glass slides.

Deparaffinized TMJ sagittal sections ($n = 6$/group) were stained with safranin-O/fast green counterstain and toluidine blue (IHC World, Woodstock, MD) to analyze cartilage thickness and proteoglycan content. Immunostaining was utilized to localize the expression of Lrp5 and sclerostin (Sost) in the MCC. Serial sagittal sections were incubated with Lrp5 and Sost primary antibodies (Aviva Systems Biology, San Diego, CA). Rinsed sections were incubated with a biotinylated secondary antibody (Vectastain Elite ABC Kit) followed by a VIP peroxidase substrate (Vector Laboratories, Inc., Burlingame, CA).

Fluorescent bone labels were analyzed on 4 μm sagittal sections of undecalcified joints ($n = 4$/group) embedded in methyl methacrylate (Sigma-Aldrich, St. Louis, MO).

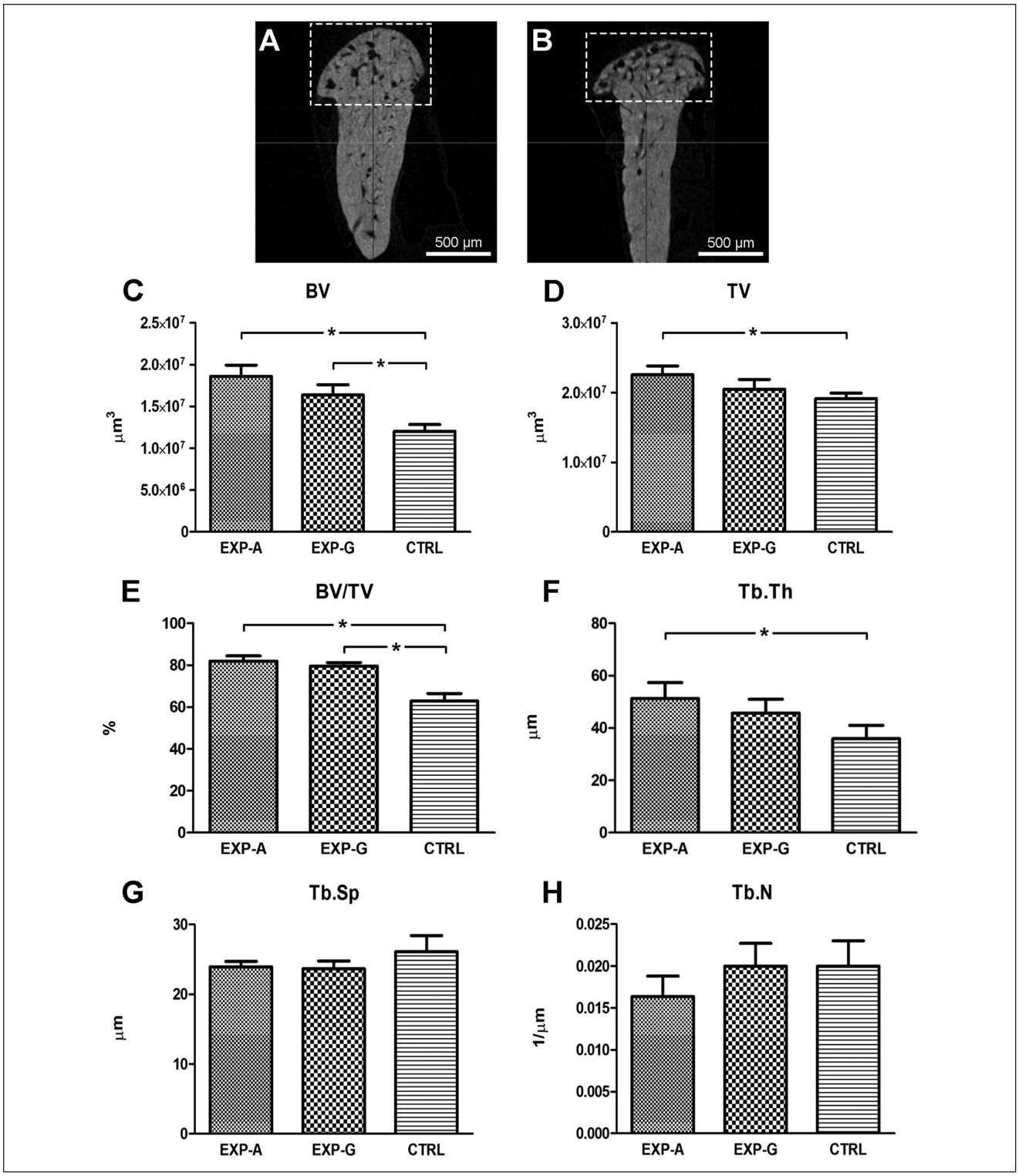

Figure 1. Temporomandibular joint (TMJ) subchondral bone changes in Lrp5-high bone mass (HBM) mice. Representative micro-computed tomography (CT) scans of the mandibular condyle from (**A**) experimental (EXP) and (**B**) control (CTRL) animals. The dotted lines denote the region of interest (ROI) in the condylar head that was used to quantify the following subchondral bone micro-CT parameters: (**C**) bone volume (BV), (**D**) total volume (TV), (**E**) percent bone volume (BV/TV), (**F**) trabecular thickness (Tb.Th), (**G**) trabecular spacing (Tb.Sp), and (**H**) trabecular number (Tb.N). Each bar on a graph represents mean ± standard error of the mean (SEM) for $n = 10$ per group. Statistically significant differences between groups are denoted by * ($P < 0.05$).

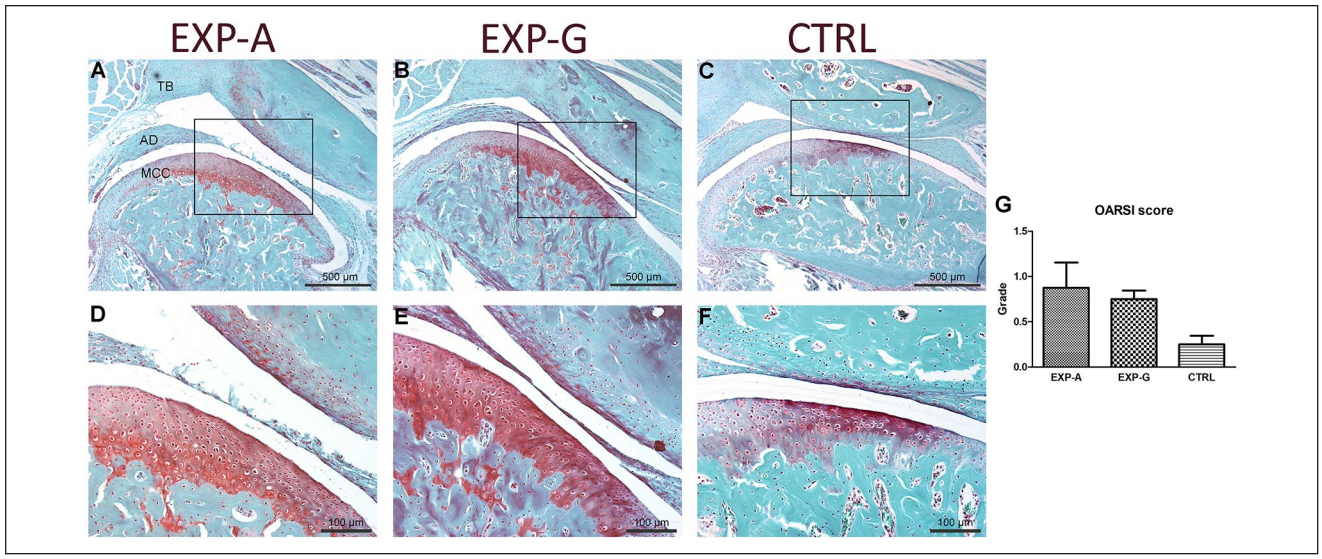

Figure 2. Histopathology grade assessment of the MCC in Lrp5-HBM mice. Safranin-O-stained sagittal histologic sections of the TMJ from (**A**) EXP-A, (**B**) EXP-G, and (**C**) CTRL groups. The black rectangle denotes the middle third of the MCC in the (**D**) EXP-A, (**E**) EXP-G, and (**F**) CTRL animals. (**G**) The Osteoarthritis Research Society International (OARSI) score was calculated from the images in panels **D** to **F**. Each bar on the graph represents mean ± standard error of the mean (SEM) for $n = 6$ per group. HBM, high bone mass; TMJ, temporomandibular joint; EXP, experimental group; CTRL, control group; TB, temporal bone; AD, articular disc; MCC, mandibular condylar cartilage.

A Nikon Eclipse Ni-U Microscope with a color camera (Nikon instruments, Melville, NY) was used to capture the histological images at 10× and 40× magnification.

Histological Analysis

Toluidine blue–stained images were used to quantify both the total cartilage area as well as the area fraction representing the proteoglycan content. Using the ImageJ software (NIH, Bethesda, MD), images were split into single channels and the entire outline of the MCC from the articular surface to the subchondral bone, was traced. A standard measurement threshold was then established for all images and the area fraction was calculated as the ratio of the positive area to the outlined MCC area.[16]

A semiquantitative histologic scoring system developed by the Osteoarthritis Research Society International (OARSI) for analyzing osteoarthritic changes in cartilage, was used to grade the safranin-O-stained sections.[17] The separation between the fluorescent bone labels was measured with ImageJ to calculate and compare the interlabel width (iL.Wi) and mineral apposition rate (MAR).

A minimum of 3 histological sections corresponding to the condylar mid-sagittal area, were used from each animal for quantification.

Statistical Analysis

All statistical analyses were performed using SPSS Statistics 20 (IBM Corporation, Armonk, NY) and GraphPad Prism (GraphPad, La Jolla, CA). Descriptive statistics were analyzed for bone volume, total volume, percent bone volume, trabecular number, trabecular separation, and trabecular thickness. The Shapiro-Wilk test was used to check the data for normality. Nonparametric Kruskal-Wallis and Mann-Whitney *U* statistical tests were used to compare the differences between the groups. The statistical significance level was set at $P < 0.05$.

Results

Micro-CT scans were used to quantify and compare the changes in the subchondral bone between the experimental and control groups. BV was significantly increased in both EXP-A and EXP-G groups compared to the CTRL group (**Fig. 1C**). TV was also increased in both experimental groups, but the difference was only significant between EXP-A and CTRL groups (**Fig. 1D**). Similar to BV, BV/TV was significantly higher in EXP-A and EXP-G compared to CTRL (**Fig. 1E**). Tb.Th was increased (**Fig. 1F**) while Tb.Sp was decreased (**Fig. 1G**) in both experimental groups compared with the control group. Tb.N showed a slight decrease in EXP-A compared with the other groups (**Fig. 1H**).

Qualitative analysis of safranin-O-stained histologic sections of the TMJ showed increased staining in the MCC in EXP-A (**Fig. 2A**) and EXP-G (**Fig. 2B**) compared with CTRL (**Fig. 2C**) animals. Anteroposteriorly, an ROI in the middle third of the MCC was compared between the groups (**Fig. 2D-F**). In the experimental animals (**Fig. 2D** and **E**) intense safranin-O staining was seen extending beyond the

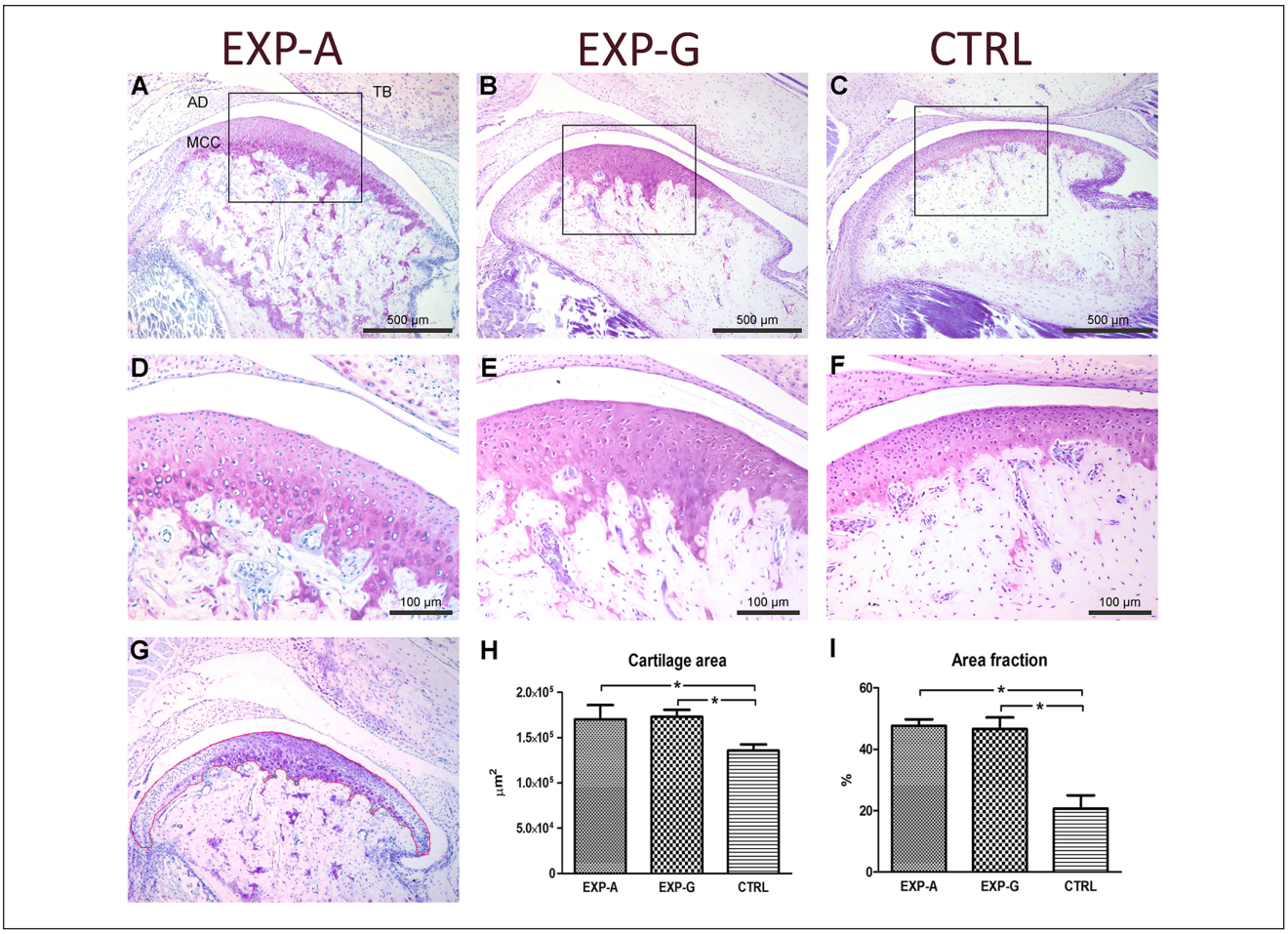

Figure 3. Increased cartilage thickness and extracellular matrix accumulation in Lrp5-HBM mice. Toluidine blue–stained sagittal histologic sections of the TMJ from (**A**) EXP-A, (**B**) EXP-G, and (**C**) CTRL groups. The black rectangle denotes the middle third of the MCC in the (**D**) EXP-A, (**E**) EXP-G, and (**F**) CTRL animals. (**G**) The boundary of the MCC was outlined as the ROI in ImageJ from the images in panels **A** to **C**. (**H**) Total cartilage area and (**I**) area fraction of the toluidine blue positive area were calculated in the ROIs. Each bar on the graph represents mean ± standard error of the mean (SEM) for $n = 6$ per group. HBM, high bone mass; TMJ, temporomandibular joint; EXP, experimental group; CTRL, control group; ROI, region of interest; TB, temporal bone; AD, articular disc; MCC, mandibular condylar cartilage.

tidemark that denotes the interface between unmineralized and mineralized cartilage, into the subchondral bone. Mild fibrillations without loss of cartilage were noted in the EXP-A group, which led to a slightly higher OARSI histologic score in both experimental groups compared with the control group (**Fig. 2G**).

Toluidine blue staining showed a trend similar to safranin-O with increased staining in EXP-A and EXP-G compared with CTRL animals that extended well beyond into the subchondral bone (**Fig. 3A-C**). Comparing the middle third ROIs, increased cellularity in the deeper layers of the MCC and increased proteoglycan accumulation were observed in the EXP-A (**Fig. 3D**) and EXP-G (**Fig. 3E**) groups compared with the CTRL (**Fig. 3F**) group. The border of the MCC was outlined in mid-sagittal histologic sections from all groups in ImageJ (**Fig. 3G**). Both total cartilage area and the toluidine blue–positive area were significantly increased in EXP-A and EXP-G compared with CTRL animals (**Fig. 3H** and **I**).

Serial sagittal sections were used for immunohistochemical localization of Lrp5 and Sost in the MCC (**Fig. 4A** and **B**). Both Lrp5 and Sost were increased in EXP-G compared to the CTRL group (**Fig. 4C-F**). This increase was noted in the articular, proliferative and chondrocytic layers of the MCC with decreasing expression in the hypertrophic cells closer to the tidemark.

Fluorescent bone labels were analyzed in sagittal sections of the TMJ. Greater separation was seen between calcein and alizarin complexone (AC-Cal) compared with alizarin and demeclocycline (Dem-AC) (**Fig. 5A**). Both the interlabel width (iL.Wi) (**Fig. 5B**) and the mineral apposition rate (MAR) (**Fig. 5C**) were increased in the EXP groups

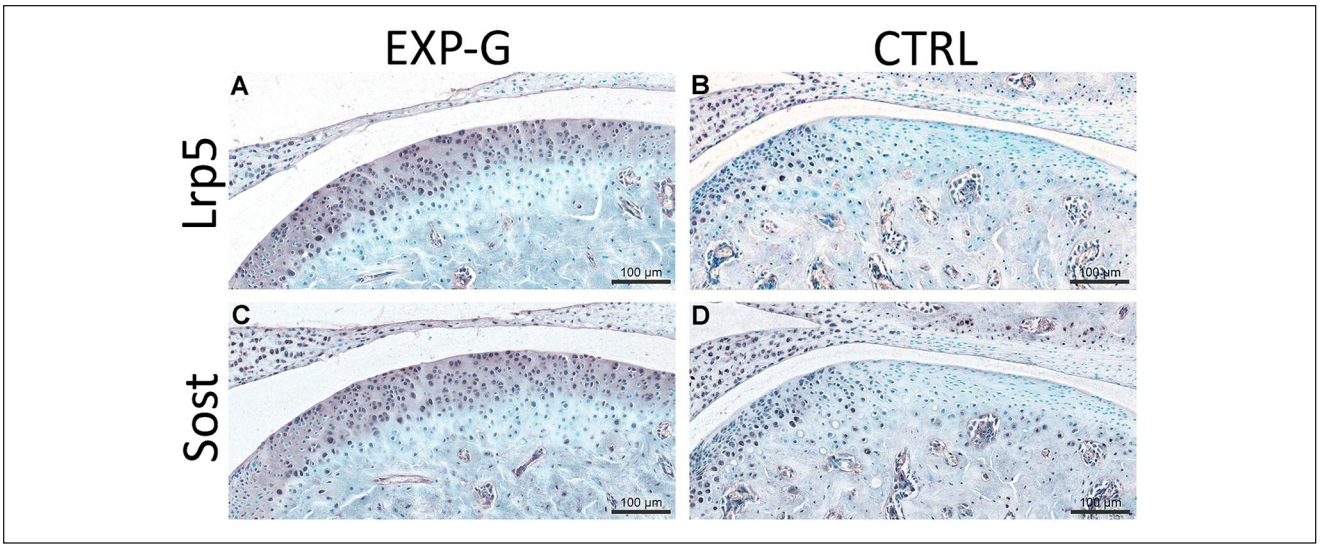

Figure 4. Increased expression of Lrp5 and sclerostin (Sost) in the MCC in Lrp5-HBM mice. Immunohistochemistry for Lrp5 (**A**, **B**) and Sost (**C**, **D**) in the middle third of serial sagittal sections of the MCC. HBM, high bone mass; MCC, mandibular condylar cartilage.

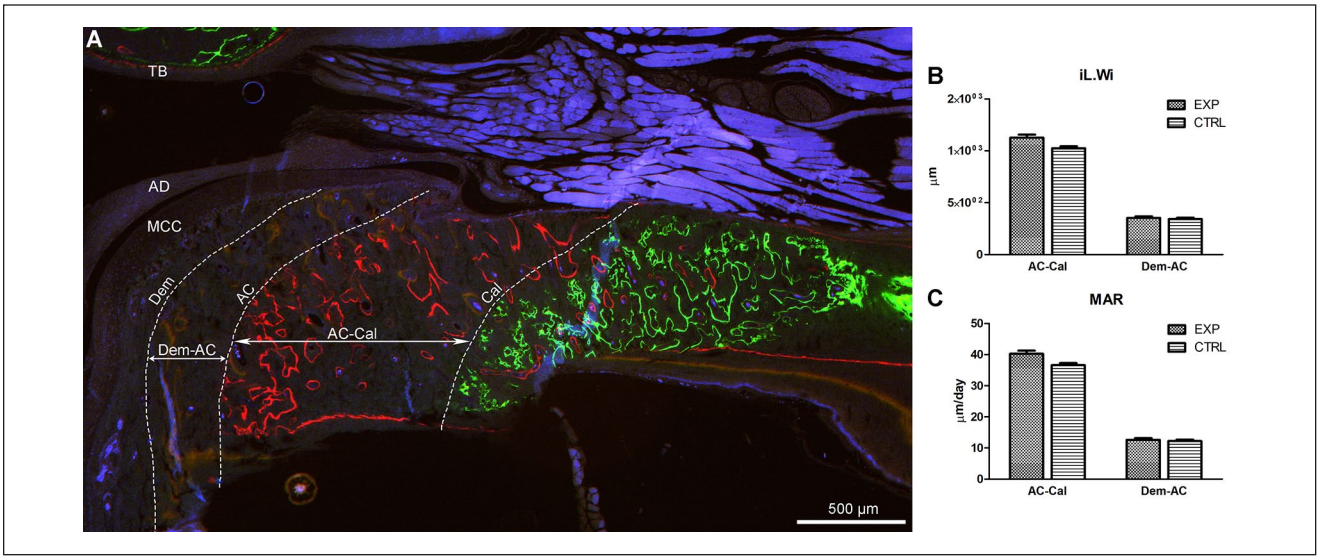

Figure 5. Subchondral bone mineralization in Lrp5-HBM mice. (**A**) Expression of fluorescent bone labels calcein (Cal; green), alizarin complexone (AC; red), and demeclocycline (Dem; yellow) in an experimental animal. (**B**) Interlabel width (iL.Wi) and (**C**) mineral apposition rate (MAR) were calculated. Each bar on the graph represents mean ± standard error of the mean (SEM) for $n = 4$ per group. HBM, high bone mass; TB, temporal bone; AD, articular disc; MCC, mandibular condylar cartilage; AC-Cal, separation between alizarin complexone and calcein; Dem-AC, separation between demeclocycline and alizarin complexone.

compared with the CTRL group. This indicated increased endochondral maturation in the Lrp5-HBM animals between the ages of 3.5 and 7.5 weeks.

Discussion

Most synovial joints develop from dedicated hyaline cartilage masses and are classified as primary cartilaginous joints. On the other hand, the MCC of the TMJ is a secondary cartilage that develops in response to functional requirements.[18] The mandibular condyle is an important growth site in the craniofacial skeleton, and the cellular organization of the MCC highlights its dual role as an articulating joint surface and growth plate cartilage. Based on cellular morphology and the expression of characteristic proteins, the MCC is divided into 4 layers.[19] The superficial articular layer is

composed of fibroblastic cells that provide protection to the joint. The underlying proliferative and cartilaginous layers are composed of osteo-chondro-progenitor cells and chondrocytes, respectively. Terminally differentiated hypertrophic chondrocytes comprise the fourth layer. During growth and function, cellular proliferation and maturation maintain the separation between the cartilaginous and bony compartments of the TMJ. However, when the functional remodeling capacity of the joint is exceeded, joint damage and subsequent osteoarthritic changes can be seen.[19]

In our study, the micro-CT parameters showed an increase in mineralized trabecular bone in the mandibular condyle from Lrp5-HBM mice. To the best of our knowledge, this is the first report of the effect of gain-of-function mutations in Lrp5 on the TMJ. Previously, similar changes were reported in the femoral and vertebral trabecular bone compartments of Lrp5-HBM mice.[20] Increased trabecular thickness and decreased trabecular spacing were also consistent in both studies. As endochondral maturation at the condyle contributes to mandibular growth, these changes in the subchondral bone could explain the enlargement of the mandible that is clinically seen in some patients with LRP5-HBM.[21,22]

We next analyzed if the changes in the bony compartment of the TMJ carried over to the cartilaginous compartment (MCC). Intense safranin-O staining suggestive of increased proteoglycan accumulation in both Lrp5-HBM groups extended through the proliferative, cartilaginous, and hypertrophic layers of the MCC. These results complement the findings of Schumacher *et al*.[23] who showed that conditional deletion of Lrp5 decreases safranin-O staining in the articular cartilage. Most of the evidence in the literature, however, suggests that Lrp5 mediates osteoarthritic cartilage destruction.[24-26] Using the OARSI histologic scoring system, we found minimal, early signs of structural changes in the MCC. The most likely reason for this is that, in the Lrp5-HBM mice, TMJ loading during routine function is within the functional adaptive remodeling capacity of the joint.[19] If either excessive external pressure is applied or as the remodeling capacity of the joint decreases with age,[27] more cartilage damage can be expected. We plan to focus on these in future studies.

We found increased cartilage thickness and proteoglycan accumulation in the MCC in both experimental groups compared with the control animals. Although there is little information in the literature about joint cartilage in Lrp5-HBM mice, our results are similar to previous studies that applied external mechanical loading to the TMJ.[16,28] In those reports, the authors attributed the expansion of the unmineralized and mineralized cartilage components to an adaptation of the MCC to the mechanical stimulus. Similar to that static loading model, we believe that the increased bone mass in the craniofacial skeleton of the Lrp5-HBM mice forms a dynamic loading model. Thus, the increase in total cartilage area as well as chondrogenic differentiation, are adaptive responses of the MCC to its altered functional demands. The irregular tidemark in the experimental group also highlights a disturbance in the delicate balance between unmineralized and mineralized cartilage in these animals.

In our study, cells in the articular, proliferative, and cartilaginous layers of the MCC demonstrated increased Lrp5 expression. Interestingly, expression of Sost, a Wnt inhibitor, was also increased and appeared to be co-localized with Lrp5. This is because the mutant Lrp5 protein that is overexpressed in the HBM mice has decreased binding affinity for Sost.[29] Thus, even though the secretion of Sost ramps up to counteract increased Lrp5, the result is an accumulation of both Lrp5 and Sost. Additionally, increased Sost expression by articular chondrocytes has been shown to protect against cartilage destruction in OA.[30] This could also explain the minimal deleterious structural changes in the articular cartilage in our study, despite the high levels of Lrp5.

Conclusion

This study demonstrates that overexpression of Lrp5 affects both the subchondral bone and the mandibular condylar cartilage of the TMJ. Increases in subchondral bone micro-CT parameters, cartilage thickness, and cartilage proteoglycan accumulation, are some of the adaptive responses of the TMJ that prevent cartilage degradation by maintaining a balance between unmineralized and mineralized cartilage. Based on these results, future research will focus on the effects of varying age, gender, and mechanical loading on the TMJ in Lrp5-HBM mice. Inflammatory mediators and bone resorption markers at the tidemark will also be analyzed.

Acknowledgments and Funding

The author(s) disclosed receipt of the following financial support for the research, authorship, and/or publication of this article: The authors acknowledge the funding provided to AU by the American Association of Orthodontists Foundation (AAOF).

Declaration of Conflicting Interests

The author(s) declared no potential conflicts of interest with respect to the research, authorship, and/or publication of this article.

Ethical Approval

All experimental procedures were performed according to a protocol approved by the Institutional Animal Care and Use Committee (IACUC).

Animal Welfare

The present study followed international, national, and/or institutional guidelines for humane animal treatment and complied with relevant legislation.

ORCID iD

Achint Utreja https://orcid.org/0000-0003-0406-2252

References

1. Gu S, Wu W, Liu C, Yang L, Sun C, Ye W, *et al*. BMPRIA mediated signaling is essential for temporomandibular joint development in mice. PLoS One. 2014;9:e101000.
2. Roberts RR, Bobzin L, Teng CS, Pal D, Tuzon CT, Schweitzer R, *et al*. FGF signaling patterns cell fate at the interface between tendon and bone. Development. 2019;146:dev170241.
3. Purcell P, Joo BW, Hu JK, Tran PV, Calicchio ML, O'Connell DJ, *et al*. Temporomandibular joint formation requires two distinct hedgehog-dependent steps. Proc Natl Acad Sci U S A. 2009;106:18297-302.
4. Serrano MJ, So S, Svoboda KK, Hinton RJ. Cell fate mediators Notch and Twist in mouse mandibular condylar cartilage. Arch Oral Biol. 2011;56:607-13.
5. Brunt LH, Begg K, Kague E, Cross S, Hammond CL. Wnt signalling controls the response to mechanical loading during zebrafish joint development. Development. 2017;144:2798-809.
6. Niehrs C. The complex world of WNT receptor signalling. Nat Rev Mol Cell Biol. 2012;13:767-79.
7. Hill TP, Spater D, Taketo MM, Birchmeier W, Hartmann C. Canonical Wnt/beta-catenin signaling prevents osteoblasts from differentiating into chondrocytes. Dev Cell. 2005;8:727-38.
8. Turner CH, Warden SJ, Bellido T, Plotkin LI, Kumar N, Jasiuk I, *et al*. Mechanobiology of the skeleton. Sci Signal. 2009;2:pt3.
9. Robling AG. The expanding role of Wnt signaling in bone metabolism. Bone. 2013;55:256-7.
10. Haudenschild AK, Hsieh AH, Kapila S, Lotz JC. Pressure and distortion regulate human mesenchymal stem cell gene expression. Ann Biomed Eng. 2009;37:492-502.
11. Sawakami K, Robling AG, Ai M, Pitner ND, Liu D, Warden SJ, *et al*. The Wnt co-receptor LRP5 is essential for skeletal mechanotransduction but not for the anabolic bone response to parathyroid hormone treatment. J Biol Chem. 2006;281:23698-711.
12. Van Wesenbeeck L, Cleiren E, Gram J, Beals RK, Bénichou O, Scopelliti D, *et al*. Six novel missense mutations in the LDL receptor-related protein 5 (LRP5) gene in different conditions with an increased bone density. Am J Hum Genet. 2003;72:763-71.
13. Niziolek PJ, Farmer TL, Cui Y, Turner CH, Warman ML, Robling AG. High-bone-mass-producing mutations in the Wnt signaling pathway result in distinct skeletal phenotypes. Bone. 2011;49:1010-9.
14. Stocum DL, Roberts WE. Part I: development and physiology of the temporomandibular joint. Curr Osteoporos Rep. 2018;16:360-8.
15. Cui Y, Niziolek PJ, MacDonald BT, Zylstra CR, Alenina N, Robinson DR, *et al*. Lrp5 functions in bone to regulate bone mass. Nat Med. 2011;17:684-91.
16. Utreja A, Dyment NA, Yadav S, Villa MM, Li Y, Jiang X, *et al*. Cell and matrix response of temporomandibular cartilage to mechanical loading. Osteoarthritis Cartilage. 2016;24:335-44.
17. Glasson SS, Chambers MG, Van Den Berg WB, Little CB. The OARSI histopathology initiative—recommendations for histological assessments of osteoarthritis in the mouse. Osteoarthritis Cartilage. 2010;18(Suppl 3):S17-23.
18. Shen G, Darendeliler MA. The adaptive remodeling of condylar cartilage—a transition from chondrogenesis to osteogenesis. J Dent Res. 2005;84:691-9.
19. Kuroda S, Tanimoto K, Izawa T, Fujihara S, Koolstra JH, Tanaka E. Biomechanical and biochemical characteristics of the mandibular condylar cartilage. Osteoarthritis Cartilage. 2009;17:1408-15.
20. Babij P, Zhao W, Small C, Kharode Y, Yaworsky PJ, Bouxsein ML, *et al*. High bone mass in mice expressing a mutant LRP5 gene. J Bone Miner Res. 2003;18:960-74.
21. Gregson CL, Wheeler L, Hardcastle SA, Appleton LH, Addison KA, Brugmans M, *et al*. Mutations in known monogenic high bone mass loci only explain a small proportion of high bone mass cases. J Bone Miner Res. 2016;31:640-9.
22. Whyte MP, McAlister WH, Zhang F, Bijanki VN, Nenninger A, Gottesman GS, *et al*. New explanation for autosomal dominant high bone mass: mutation of low-density lipoprotein receptor-related protein 6. Bone. 2019;127:228-43.
23. Schumacher CA, Joiner DM, Less KD, Drewry MO, Williams BO. Characterization of genetically engineered mouse models carrying Col2a1-cre-induced deletions of Lrp5 and/or Lrp6. Bone Res. 2016;4:15042.
24. Shin Y, Huh YH, Kim K, Kim S, Park KH, Koh JT, *et al*. Low-density lipoprotein receptor-related protein 5 governs Wnt-mediated osteoarthritic cartilage destruction. Arthritis Res Ther. 2014;16:R37.
25. Papathanasiou I, Malizos KN, Tsezou A. Low-density lipoprotein receptor-related protein 5 (LRP5) expression in human osteoarthritic chondrocytes. J Orthop Res. 2010;28:348-53.
26. Wang Y, Fan X, Xing L, Tian F. Wnt signaling: a promising target for osteoarthritis therapy. Cell Commun Signal. 2019;17:97.
27. Chen PJ, Dutra EH, Mehta S, O'Brien MH, Yadav S. Age-related changes in the cartilage of the temporomandibular joint. Geroscience. 2020;42:995-1004.
28. Kaul R, O'Brien MH, Dutra E, Lima A, Utreja A, Yadav S. The effect of altered loading on mandibular condylar cartilage. PLoS One. 2016;11:e0160121.
29. Semenov MV, He X. LRP5 mutations linked to high bone mass diseases cause reduced LRP5 binding and inhibition by SOST. J Biol Chem. 2006;281:38276-84.
30. Chan BY, Fuller ES, Russell AK, Smith SM, Smith MM, Jackson MT, *et al*. Increased chondrocyte sclerostin may protect against cartilage degradation in osteoarthritis. Osteoarthritis Cartilage. 2011;19:874-85.